Remote sensing of aerosol optical characteristics in sub-Sahel, West Africa

G. Pandithurai,[1,2] R. T. Pinker,[1] O. Dubovik,[3,4] B. N. Holben,[3] and T. O. Aro[5]

Abstract. We have determined the characteristics of sub-Sahelian aerosols from a 2-year record of continuous ground-based measurements, made at the University of Ilorin, Ilorin (08°19′N, 04°20′E), Nigeria, in cooperation with the Aerosol Robotic Network. Observations of spectral aerosol optical depths during the dusty harmattan season indicate more than a twofold increase, when compared to other seasons. Retrieved columnar volume size distributions show the existence of bimodality with a dominant coarse mode. The retrieved size distributions were grouped according to different ranges of aerosol optical depths to characterize the aerosols for this particular region. Monthly means of retrieved single-scattering albedos show a sharp decrease from ~0.95 to ~0.85 at 500 nm from the preharmattan to the harmattan season when biomass burning is also practiced, increasing the presence of absorbing aerosols. On the basis of these comprehensive observations, we propose to augment existing desert aerosol models, as presented in the literature, to better characterize the dust outbreak season in West Africa, which is quite prolonged and overlaps with the biomass burning season.

1. Introduction

It has been observed that each year, between November and March, a large amount of dust is transported over Nigeria to the Gulf of Guinea [*Kalu*, 1979]. The cold and dry wind, which is the main agent for this dust transport is known as the "harmattan." During this season, the atmosphere over this region is characterized by high dust levels, relatively high daytime and low nighttime temperatures, dry and weathering vegetation, high incidence of forest fires, and poor visibility. The harmattan aerosols have been known to have adverse health affects, such as causing acute respiratory infections, pneumonia, and bronchitis, as documented for northern Nigeria, where the effect is most severe, by *Adefolalu* [1984] and *Adedokun et al.* [1989]. The atmospheric haze and the occasional early morning/evening fogs due to northward incursions of moist southwesterly winds lead to frequent cancellation of flights, resulting in a heavy loss of revenue [*Adefolalu*, 1984]. Moreover, the "harmattan haze" is a threat to safety of civil aviation. Out of the 11 air disasters in Nigeria and the Ivory Coast during the period November 1969 to January 2000 (http://www.airdisasters. co.uk/Disasters.htm), 10 occurred during the harmattan season. The harmattan dust episode of January 30, 2000, and the corresponding optical parameters as observed at the Ilorin site are discussed by *Pinker et al.* [2001]. The harmattan dust haze is a well-known phenomenon and was first investigated using visibility data [*Adebayo*, 1989; *McTainsh*, 1980]. Chemical char-

acterization of harmattan dust was also carried out [*Cox et al.*, 1982; *Adedokun et al.*, 1989; *Afeti and Resch*, 2000]; however, a complete optical characterization of the harmattan aerosols and long-term remote measurements are almost nonexistent.

Recently, it has been speculated that since the onset of the droughts that started in the 1970s, the Sahel is the major source region of wind-borne dust, contrary to earlier belief that it is the Sahara desert [*N'Tchayi Mbourou et al.*, 1994, 1997]. *Nicholson* [2000] reported that (1) there has been a steady increase in the frequency of occurrence of dust conditions at the surface over West Africa since the early 1970s, (2) an increase in dust occurrence has paralleled a decrease in rainfall, and (3) the length of the season with dusty conditions has steadily increased.

Several studies suggest that dust aerosol has a significant impact on meteorological processes [*Karyampudi and Carlson*, 1988; *Chang*, 1993; *Alpert et al.*, 1998]. General circulation (GCM) studies [*Tegen and Miller*, 1998] have shown that regional climate cannot be realistically simulated without introducing dust mobilization in the model, and models have shown that the dust has an impact on synoptic conditions and therefore on rainfall [*Tegen and Fung*, 1994; 1995]. Hence long-term measurements of dust characteristics are needed in climate research.

In this paper we document the annual variation of aerosol optical characteristics obtained from 2 years of ground-based measurements, which were made as part of a NASA Earth Observing System (EOS) validation program, within the framework of the Aerosol Robotic Network (AERONET).

2. Experimental Site and Data

The experimental site is located on the campus of the University of Ilorin, Ilorin, Nigeria (08°19′N, 04°20′E, 350 m above mean sea level (amsl)), at the upper tip of the Guinea savannah zone in the sub-Sahel, under the influence of the annual oscillation of the Intertropical Convergence Zone (ITCZ). During the "dry season" (November–March) the prevailing northeasterly wind, known as "harmattan," brings in air containing Saharan dust from the Chad basin when a large amount

[1]Department of Meteorology, University of Maryland, College Park, Maryland, USA.
[2]Indian Institute of Tropical Meteorology, Pune, India.
[3]Laboratory for Terrestrial Physics, NASA Goddard Space Flight Center, Greenbelt, Maryland, USA.
[4]Also at Science Systems and Applications, Inc., Lanham, Maryland, USA.
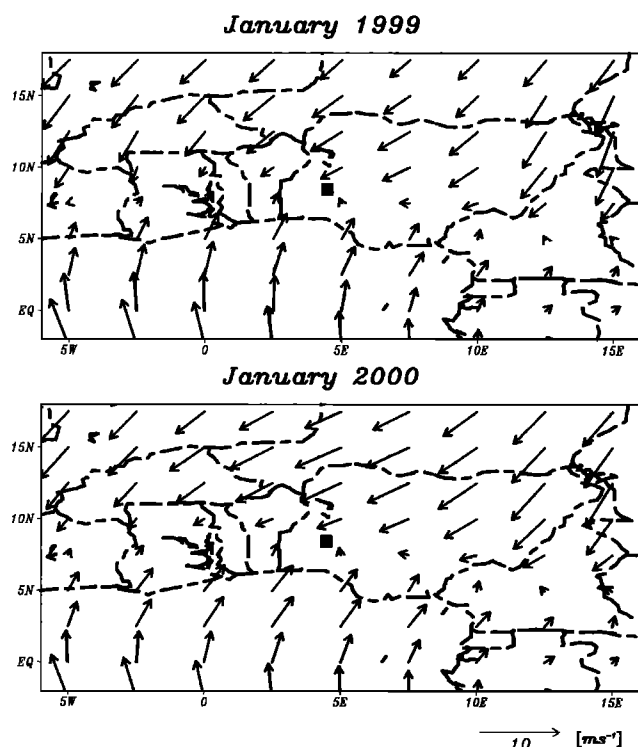[5]University of Ilorin, Ilorin, Nigeria.

Figure 1. NCEP reanalysis of surface winds over West Africa for January 1999 and 2000.

of dust particles is transported in a plume downwind from the source region by the strong northeasterly winds mainly at the 900 and 850 mbar levels north of the ITCZ, taking a southwesterly trajectory over Nigeria [*Kalu*, 1979]. In this season, dust plumes can have a thickness of up to 3 km, vary strongly in aerosol content, and reduce the visibility to less than 1 km. Harmattan winds are the main mechanism for dust transport and produce severe winter weather conditions in West Africa, known as the "harmattan haze." During the "wet season" (April–October), conditions are typified by moist maritime southwesterly flow from the Gulf of Guinea over West Africa. Figure 1 shows the average surface wind flow patterns as provided by the National Center for Environmental Prediction (NCEP), Numerical Weather Prediction (NWP) model analysis for January 1999 and 2000. As evident, the intensity of the northeasterly flow in January 2000 was much stronger than a year before.

Measurements of aerosol optical depths at this site started in 1987 [*Pinker et al.*, 1994], measurements of surface radiative fluxes started in 1992 [*Miskolczi et al.*, 1997] and were upgraded in May 1995, under the NASA EOS Validation Program. The site is being continuously upgraded to meet the requirements of the World Climate Research Programme (WCRP) Baseline Surface Radiation Measurement (BSRN) Network [*Ohmura et al.*, 1998]. The radiation observations made at the site are archived at the World Radiation Data Center (WRDC) located at the Eidgenossische Technische Hochschule (ETH), Zurich, Switzerland. Observations of aerosol optical properties at Ilorin, Nigeria, have been upgraded in May 1998, as part of the Aerosol Robotic Network (AERONET) activity, in support of current and future satellite missions such as the Clouds and Earth Radiant Energy System (CERES), the Moderate-Resolution Imaging Spectroradiometer (MODIS), and the Na-

tional Space Development Agency (NASDA) of Japan, ADEOS-II mission.

The instrument used in the present study to monitor aerosol properties is a CIMEL sky radiometer, of the type used in the Aerosol Robotic Network (AERONET), which is a worldwide-federated network operated at numerous climatically important regions and led by the NASA Goddard Space Flight Center [*Holben et al.*, 1998]. The instrument is an automatic Sun-tracking sky radiometer capable of measuring both Sun and sky radiance at eight spectral channels. The filters are centered at wavelengths 340, 380, 440, 500, 670, 870, 940, and 1020 nm, located in a filter wheel, which is driven by a stepper motor. The observations are transmitted almost in real time via the European Meteosat (D. Tanre, private communication, 1997). Detailed information on measurement protocol, radiometric precision, calibration procedures, and processing methods are described by *Holben et al.* [1998]. Data used in the present study utilize direct solar and sky radiance in the almucantar from April 1998 to March 2000. The CIMEL sky radiometer optical head has been replaced with a recalibrated one in August 1999 in order to meet the AERONET maintenance schedule.

3. Results and Discussion

3.1. Spectral Aerosol Optical Depth

Time series of aerosol optical depths at 500 nm and monthly means at all the wavelengths are shown in Figures 2 and 3a, respectively. Optical depths during December to March for both years are higher when compared to other months. This is due to the dust outbreaks (natural) and biomass burning events (anthropogenic) most common during the dry season at the observational site. A strong spectral dependence in aerosol optical depths (AODs) is also evident. This suggests that aerosols from biomass burning are present during the dry season and are significant. The day-to-day variability of aerosol optical depth was considerably higher during the dry season than during the other seasons, due to dust and biomass burning events. In the past, *N'Tchayi Mbourou et al.* [1994, 1997] used visibility data to examine the spatial and temporal distribution of dust over West Africa. From those studies it was evident that there has been a steady buildup of dust over West Africa since the early 1970s, and it is consistent with the increased trend in African dust as measured at sites downstream [*Carlson and Prospero*, 1972]. While there are several source areas for dust aerosols, the area of Bilma (Niger) and Faya Largeau (Chad) are the main source regions for dust over Nigeria [*Wilson,*
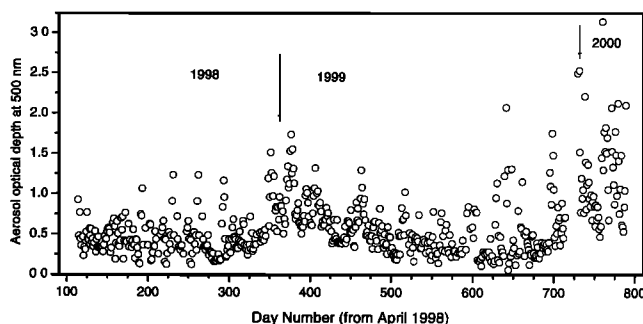

Figure 2. Time series of daily mean aerosol optical depths at 500 nm as observed at Ilorin, Nigeria.
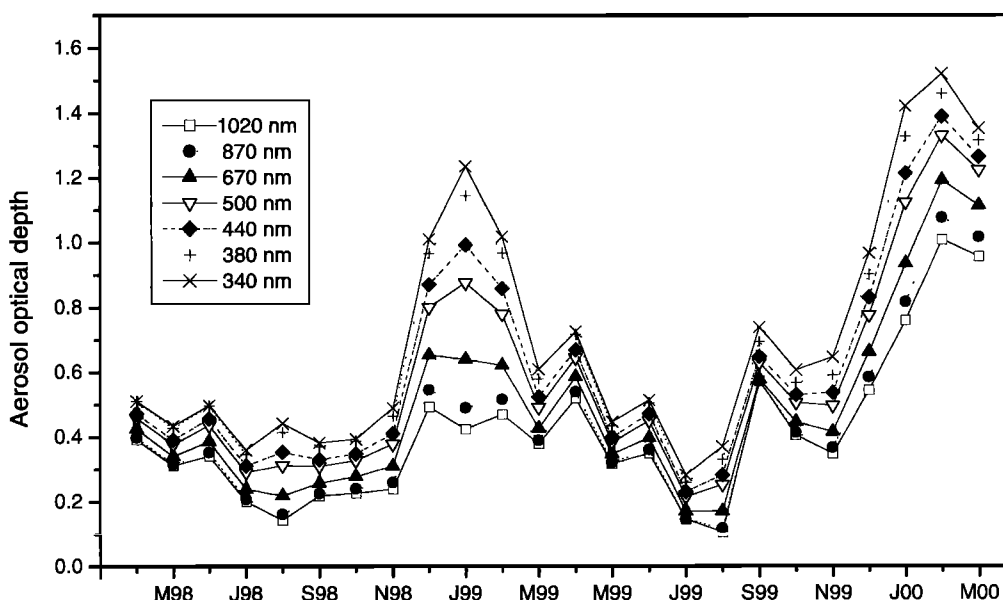
Figure 3. Month-to-month variation in spectral aerosol optical depths (in seven spectral intervals) as observed at Ilorin, Nigeria, during April 1998 to March 2000.

1971; *Kalu*, 1979]. In summer, AODs are found to be lower over Nigeria when dust aerosols follow a trajectory over southern Algeria, Morocco, and across the Atlantic to the Caribbean Islands [*Martin*, 1975; *Prospero*, 1999].

In Figure 4 a comparison of the intensities of direct shortwave radiation, as measured with an Eppley Normal Incidence Pyrheliometer during two different days in the harmattan season, is presented. The top panel is for a high-aerosol loading

Figure 4. Diurnal variation of normal incidence shortwave radiation and aerosol optical depths (at 500 nm) during high- and low-aerosol loading days.

case (τ_a (500 nm) ~1.3) when the maximum normal incidence shortwave radiation was only 400 W m^{-2}. The bottom panel is for a relatively low-aerosol loading case (τ_a (500 nm) ~0.8) when normal incident shortwave radiation reached as much as 600 W m^{-2}. This is to illustrate the drastic radiative effects during high-aerosol loading days, which are frequent during the harmattan season.

3.2. Intraseasonal Variation in Spectral Aerosol Optical Depth and Precipitable Water Vapor

To study the intraseasonal variation in spectral aerosol optical depths and in precipitable water vapor, the observations were grouped into four seasons, as shown in Figure 5. There is a significant increase in aerosol optical depth and strong spectral dependence during December–March, as compared to the other seasons. Aerosol optical depths remained almost constant during the other seasons, but there was an increase in spectral AODs in 1999–2000 as compared to 1998–1999. Precipitable water vapor, as derived from the CIMEL observations in the spectral channels 870 and 940 nm, also shows a systematic seasonal variation, high during June–August and low during December–February. The precipitable water vapor as available from the NCEP reanalysis data is shown along with the CIMEL-derived values for comparison. Spectral AODs during the preharmattan season (SON) depend strongly on the start of the biomass burning of the savannahs. Interannual variation of AODs suggest that the length of the season with dusty conditions is longer in the 1998–1999 harmattan as compared to the 1999–2000 harmattan season.
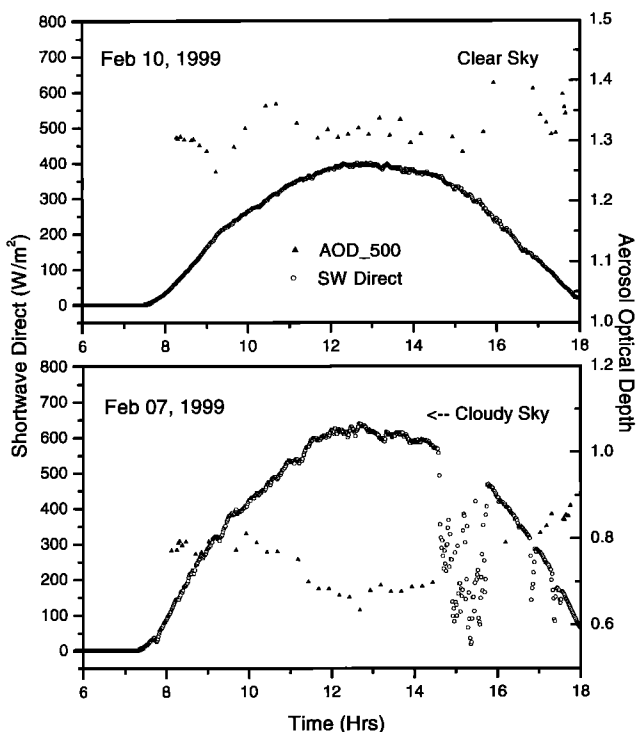
3.3. Size Distribution

The spectral dependence of AOD contains information about the size of the particles [*Junge*, 1955; *Rangarajan*, 1972; *Pandithurai et al.*, 1997; *Remer et al.*, 1999]. The Angstrom exponent α, which is a measure of the size distribution, can be obtained by fitting a power law to the aerosol optical depths and wavelength [*Eck et al.*, 1999; *Reid et al.*, 1999], as given in the following expression:
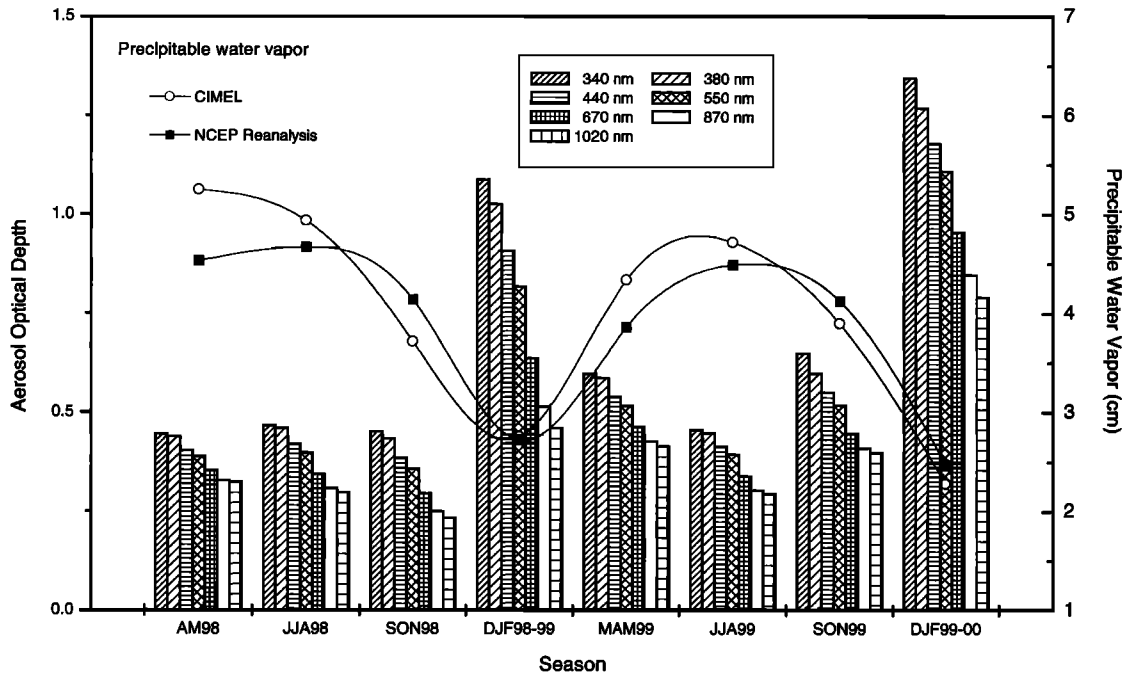
Figure 5. Intraseasonal variation of spectral aerosol optical depths and precipitable water vapor, as observed at Ilorin, Nigeria. Precipitable water was derived both from the CIMEL sky radiometer observations and from the NCEP reanalysis.

$$\tau_a(\lambda) \propto \lambda^{-\alpha}.$$

Angstrom exponents computed from such spectral dependence were grouped into monthly means and are shown in Figure 6. In general, the exponent is higher when there is a relative dominance of small particles. The monthly mean values of the Angstrom exponent show higher values during both July–September and November–January. The larger number of accumulation mode particles observed during November–January is due to aerosols from biomass burning.

Size distributions were retrieved using a radiative transfer algorithm developed by *Dubovik and King* [2000]. Optical characteristics of aerosols such as optical thickness, phase function, and single-scattering albedo are modeled from microstructure parameters using the following approximations:

Figure 6. Month-to-month variation in Angstrom exponent as observed at Ilorin, Nigeria, during April 1998 to March 2000.

$$\tau_{ext}(\lambda) P(\theta; \lambda) = \int_{r_{min}}^{r_{max}} K_{scat}(\theta, \lambda, m, r) n(r) \, dr,$$

where K_{scat} is a scattering cross section, $P(\theta, \lambda)$ is the phase function, and $n(r)$ denotes particle number size distribution. Aerosols are assumed to be spherical particles and approximated by Mie functions derived for spherical and homogeneous particles with a complex refractive index $m(\lambda)$. Volume size distributions were retrieved using a detailed radiative transfer Sun-sky radiance algorithm by *Dubovik and King* [2000]. More details on the procedure and about the accuracy of the retrieved aerosol optical properties can be found in the work of *Dubovik et al.* [2000].

The retrieved volume size distributions generally represent bimodal or trimodal distributions. About 135 retrieved size distributions were grouped as a function of aerosol optical depth. Figure 7 illustrates the aerosol size distributions as a function of AOD at 670 nm. A bimodal distribution is evident, and for intermediate optical depth values, a secondary coarse mode is present. In general, mode radii decrease for increasing optical thickness values during the harmattan season dust episodes, accumulation mode radii shift from 0.10 to 0.07 μm, and coarse mode radii vary from 2.0 to 4.0 μm. Characterizing particles as spherical introduce biases, namely, the appearance of an artificially high mode of small particles in sizes smaller than 0.1 μm may be an artifact of nonsphericity.
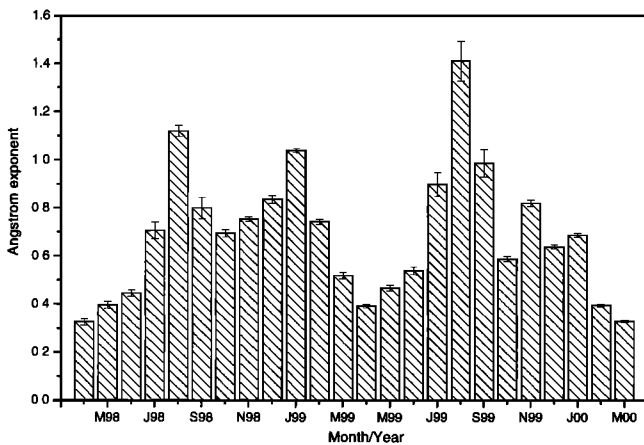
3.4. Single-Scattering Albedo

Single-scattering albedo (ω_0) of atmospheric aerosols is an important parameter for obtaining accurate estimates of the Earth's radiative budget. Procedures to retrieve ω_0 are not yet well established due to the limited information content of optical measurements. The inversion method used in this study
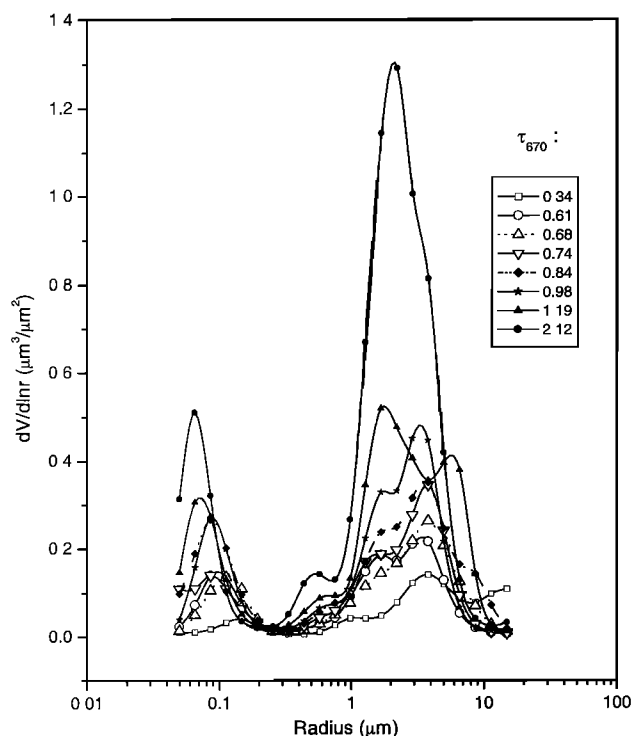
Figure 7. Proposed size distribution model for different values of aerosol optical depth.

Figure 9. Single-scattering albedo ω_0 as a function of the Angstrom exponent for wavelengths 440, 670, 870, and 1020 nm.

allows global fitting of spectral and multiangle Sun/sky radiance with a simultaneous search for the size distribution and complex refractive index. Accuracy assessments of the inversion code by *Dubovik et al.* [2000] indicate that the error in retrieved ω_0 is smaller for higher optical thickness, ~0.03 for τ_a (440 nm) $\geq$ 0.5, and for solar zenith angles greater than 45°. Because optical thickness is high over Ilorin, Nigeria, throughout the year, and since the recommended criteria for solar zenith angles were applied, the expected errors in the retrieved ω_0 are low.

In the retrieval process, the aerosol particles are assumed to be polydispersed homogeneous spheres with the same complex refractive index. Tests have shown that the assumptions of homogeneous spheres with an effective complex index of refraction allow both the accurate fitting of the majority of actual
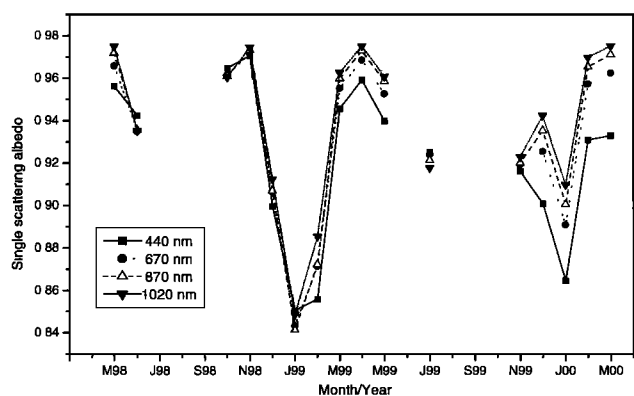
observations of atmospheric radiance and the appropriate modeling of the main radiative effects of the aerosol (absorption and scattering). The current estimates of accuracy for desert dust or other aerosol dominated by coarse particles are as follows: $dV(r)/\ln r$, 15–25% for $r \geq 0.5$ μm; $\omega_0(\lambda)$, 0.03; $k(\lambda)$, 50%; $n(\lambda)$, 0.05.

If the nonsphericity assumption is not satisfied, it is possible to obtain nonrealistically high fine mode with maximum at $r < 0.1$ μm. This effect is at a maximum for high solar zenith angles and at a minimum for low solar zenith angles (20°–30°).

Monthly and seasonal mean values of spectral ω_0 are shown in Figure 8. To increase the reliability of the retrieval, only observations for which solar zenith angles were greater than 45° were used. This resulted in missing values for some months. The spectral dependence of ω_0 shows increasing values with an increase in wavelength, and a reverse wavelength dependence of ω_0 can be noted in the dry season, which is due to the dominance of absorbing aerosols from biomass burning. Seasonal means of ω_0 indicate low values (<0.9) during DJF of 1998–1999 and 1999–2000. Lower values of ω_0 during SON of 1999 are due to the early start of biomass burning in the vicinity of the observing station. Differences between the spectral dependence of ω_0 of DJF of 1998–1999 and DJF of 1999–2000 indicate the dominance of dust aerosols during January

Figure 8. Month-to-month variation in spectral single-scattering albedo as observed at Ilorin, Nigeria, during April 1998 to March 2000.
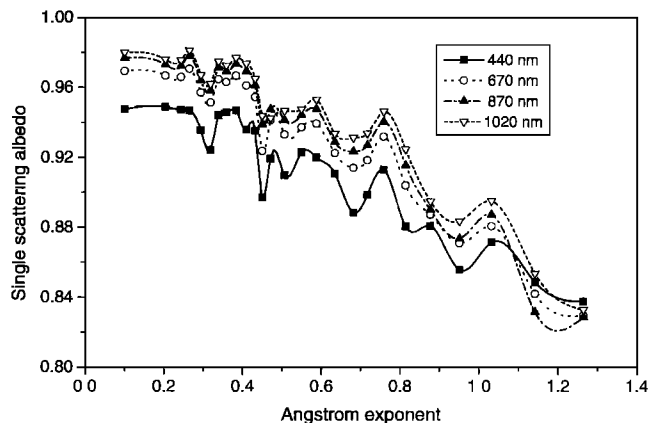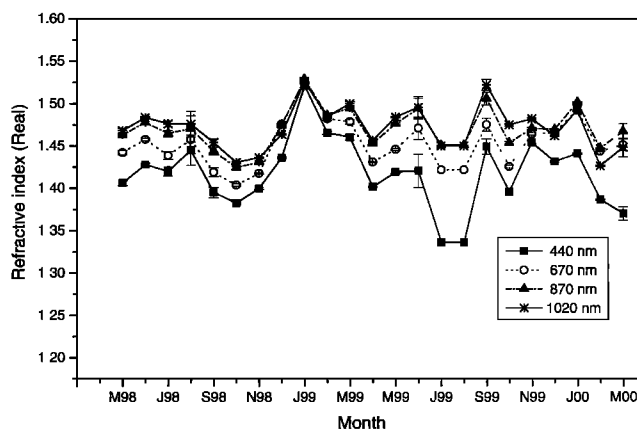

Figure 10. Month-to-month variation of the real part of the refractive index.
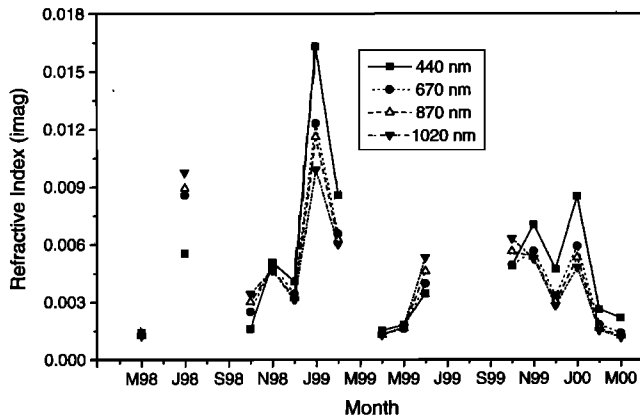
Figure 11. Month-to-month variation of the imaginary part of refractive index.

Figure 13. Comparison of CIMEL-derived aerosol optical depths at 670 nm and the NOAA 14 AVHRR operational aerosol optical depth [*Stowe et al.*, 1997].

and February 2000. Frequency distribution of single-scattering albedo at all four wavelengths indicates a modal value of >0.95 (mostly of scattering aerosols), but the 2-year mean (<0.9) suggests an absorbing type of aerosols (biomass burning). Variable elemental ratios reflect variable mineralogical composition of soils. Dust in the Sahelian region is characterized by a high Fe/Al ratio due to abundance of ferralitic soils in the Sahel [*Sokolik and Toon*, 1999]. In Figure 9 the single-scattering albedo is presented as a function of the Angstrom exponent. As evident, several distinct sections can be identified in this figure, starting with relatively higher values of ω_0 above 0.95 at low values of the Angstrom exponent, characteristic of dust, and gradually decreasing toward lower values of ω_0 at higher values of the exponent, characteristic of a higher concentration of aerosols from biomass burning, indicating clearly that dust is much less absorbing than aerosols emanating from the burning of biomass.

3.5. Complex Refractive Indices

The aerosol refractive indices are determined by the physical and chemical properties of the aerosol, namely, in terms of the
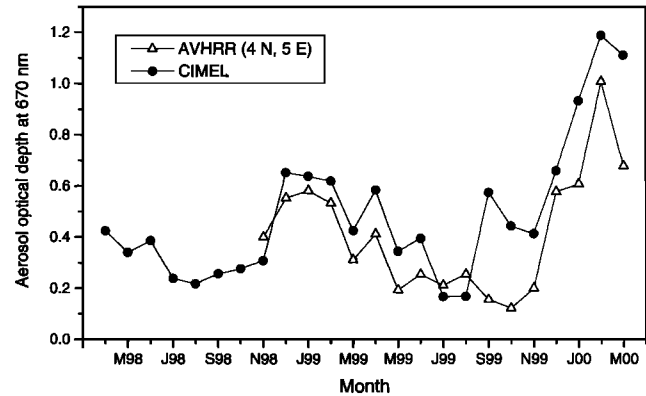
generation mechanisms and composition of the aerosol. The bulk optical properties of the aerosols may be represented by a complex index of refraction ($m = n_{real} - in_{imag}$) which is a function of wavelength in both visible and infrared regions of the spectrum. The concepts for determining aerosol refractive indices from multiangular radiance measurements are based on the principle of partial separation of the effects of refractive index and size distribution on the angular variability of sky radiance [*Wendish and von Hoyningen-Huene*, 1994; *Yamasoe et al.*, 1998]. The retrieval method of *Dubovik and King* [2000], used in the present study, implements retrieval via simultaneous fitting of radiances measured in the entire available angular and spectral range and thus can improve retrieval accuracy. A sufficiently accurate retrieval of aerosol single-scattering albedo and complex index of refraction are possible only for high-aerosol AOD. On the basis of a sensitivity study [*Dubovik et al.*, 2000] it was found that the AOD at 440 nm should be larger than 0.2. This condition is satisfied in the present study.

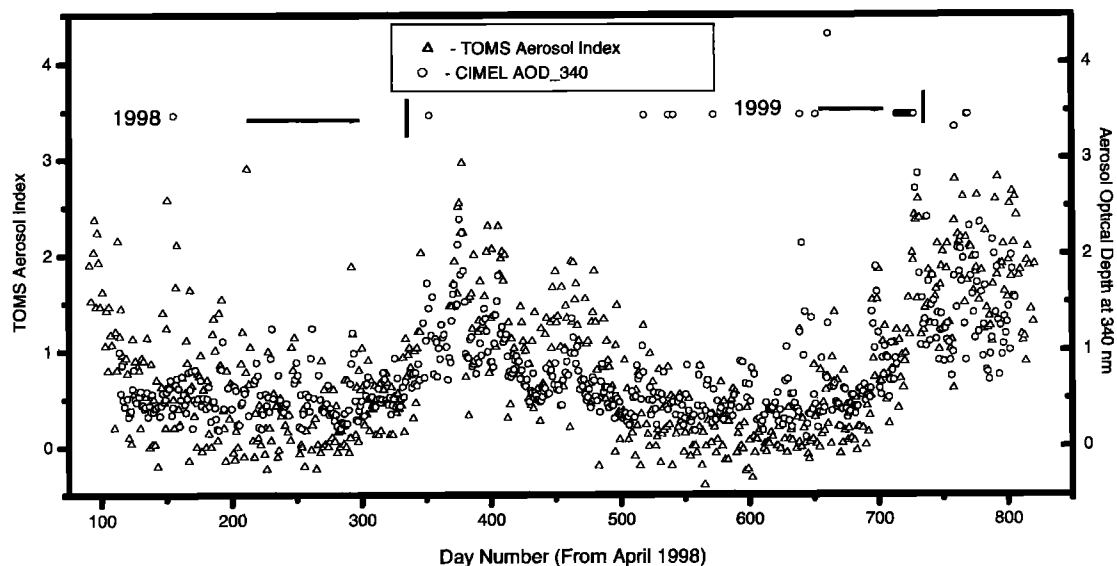The retrieved real and imaginary refractive indices were

Figure 12. Comparison of CIMEL-derived aerosol optical depths at 340 nm and TOMS-derived aerosol index for a 2-year period [*Herman and Celarier*, 1997].

Table 1. Sub-Sahelian Aerosol Model[a]

Season	τ_a (440)	τ_a (500)	τ_a (670)	τ_a (870)	τ_a (1020)	PWV, cm
Harmattan	0.895	0.830	0.695	0.602	0.558	2.787
(Nov.–March)		0.59[b]	0.653[c]			2.76[c]
		0.29[f]	0.485[e]			1.35[d]
		0.333[g]				1.13[e]
Nonharmattan	0.476	0.455	0.405	0.372	0.363	4.620
(April–Oct.)		0.431[b]	0.704[e]			2.75[d]
		0.19[f]				3.84[e]
		0.273[g]				

[a]Spectral aerosol optical depths and precipitable water vapor information.
[b]d'Almeida [1987], measurements made at Zaria, Nigeria, during 1981–1982.
[c]Faizoun et al. [1994], measurements made at Ouangofitini during 1985–1987.
[d]Tuller [1968].
[e]Faizoun et al. [1994], measurements made at Bidi during 1987–1989.
[f]Tegen et al. [1997], obtained from monthly mean totals of nine individual species, derived from transport models, in a grid cell over Ilorin, Nigeria.
[g]Values from the Global Aerosol Data Sets (GADS) by Koepke et al. [1997] for winter (0% RH) and summer (70% RH), at 500 nm over a 10°N, 5°E grid box.

grouped into monthly means and are shown in Figures 10 and 11. Monthly means of the real part of the refractive index show a gradual decrease during the wet season. Starting from November, there is an increase in these values, peaking in January. The artificial spectral dependence observed in the real part of refractive index is mainly due to nonsphericity errors, and therefore only values for 870 and 1020 nm should be used. The frequency distribution of the real refractive indices gives a mean value of 1.46 at 670 nm, which is in agreement with refractive indices of quartz and silicates [Krekov, 1993]. Mineralogical analysis of the harmattan dust indicated that it is predominantly composed of quartz (>70%) followed by microcline, kaolinite, and traces of mica and halloysite; chemical analyses indicated a predominance of SiO_2 (>60%) [Adedokun et al., 1989].

Monthly means of imaginary refractive indices also show significant seasonal variation with high values in the dry season (more absorbing aerosols, such as mineral dust and biomass) and low values in the wet season (scattering-type water soluble). Interannual variations show a significant spectral dependence during the 1999–2000 harmattan season. A statistical analysis of retrieved imaginary refractive indices over Ilorin, Nigeria, yields a mean value of 0.0065 at 670 nm. Lindberg and Laude [1974] measured n_{imag} as a function of wavelength for desert dust at visible and near-infrared wavelengths by diffuse reflectance spectroscopy, and their values decreased from ~0.01 at 400 nm to ~0.006 at 600 nm. Lindberg and Gillespie [1977] reported that the larger soil particles, those with aerodynamic radii >5.5 μm, showed significantly less absorption than the smaller particles, reflecting on differences in composition. It is evident from our observations that the imaginary refractive indices are found to be low during the dust storm episodes. The seasonal means indicate high imaginary refractive indices during the dry season, which is dominated by biomass burning events and soil dust transport to the site [Nicholson, 2000; Kalu, 1979].

3.6. Comparison With TOMS and AVHRR Data

Ground-based remotely sensed aerosol data over this region can be used to evaluate existing space-based aerosol retrievals, such as those from TOMS [Herman and Celarier, 1997; Torres et al., 1998] and AVHRR [Stowe et al., 1997; Nakajima and Higurashi, 1998; Chowdhary et al., 2001] and for future valida-

tion of retrieved values from recently launched instruments, such as the EOS MODIS on the TERRA mission [King et al., 1992]. To compare the ground measurements with the TOMS aerosol index, which is derived mainly from the 340 and 380 nm reflectances, CIMEL-observed aerosol optical depths at 340 nm were grouped into daily means for 2 years (from April 1998 to March 2000). TOMS aerosol index over Ilorin, Nigeria, was computed by taking weighted means from four neighboring grids of 1° spatial resolution. A comparison of daily mean AOD at 340 nm and TOMS aerosol index is shown in Figure 12, illustrating good agreement in the detection of the dust outbreak.

Monthly means of analyzed aerosol optical depths at the closest ocean grid (4°N, 5°E) to Ilorin (08°19'N, 04°20'E), Nigeria, is shown in Figure 13, along with CIMEL-derived AODs at 670 nm. The NOAA operationally retrieved AODs compare well with the nearest ground-based measurements, being slightly lower, as should be expected. The possible differences may be due to excess cloud screening in the NOAA product, or the difference in distance between the two sites. The much higher values observed during November 1999 over Ilorin may be due to local biomass burning effects.

3.7. "Sub-Sahelian Dust" Aerosol Model

Desert aerosols have large variability in their physical and optical properties, when compared to other types of aerosols. Generally, during the winter season, the aerosols are considered as desert background aerosols, and those during the summer season are termed as wind carried [d'Almeida, 1987]. This is not the case over sub-Sahel. Dust mobilization occurs over

Table 2. Sub-Sahelian Aerosol Model[a]

Season	ω_0 (440)	ω_0 (670)	ω_0 (870)	ω_0 (1020)
Harmattan	0.880	0.887	0.887	0.889
	0.71[b]	0.75[b]	0.72[b]	
	0.71[c]	0.92[c]		
Nonharmattan	0.929	0.932	0.935	0.938
	0.75[b]	0.79[b]	0.83[b]	

[a]Single-scattering albedo.
[b]d'Almeida [1986, 1991].
[c]Carlson and Caverly [1977].

Table 3. Sub-Sahelian Aerosol Model[a]

Season	Ref Index (440) Real	Imag	Ref Index (670) Real	Imag	Ref Index (870) Real	Imag	Ref Index (1020) Real	Imag
Harmattan	1.436	0.0085	1.468	0.0074	1.475	0.0075	1.470	0.0077
		0.01[b]		0.004[b]				
				0.008[c]				
		0.01[d]		0.006[d]				
	1.525[e]	0.005[e]						
Nonharmattan	1.405	0.0036	1.434	0.0039	1.457	0.0042	1.465	0.0044

[a]Real and imaginary refractive indices.
[b]*Patterson et al.* [1977].
[c]*Carlson and Caverly* [1977].
[d]*Lindberg and Laude* [1974].
[e]*Grams et al.* [1974].

sub-Sahel during the winter due to favorable meteorological conditions, such as the harmattan wind. As such, a dust aerosol model, characteristic of the Sahelian conditions, could augment existing dust models and better fit the conditions in this region. Moreover, during the dry winter conditions in this region, biomass burning is practiced and has a strong effect on the optical properties of the aerosols. The 2-year record of continuous observations of direct Sun and diffuse sky measurements made at this site serves for constructing a preliminary sub-Sahelian dust model that describes more closely conditions in this region than the available desert aerosol models found in the literature.

The proposed characteristics for the sub-Sahelian aerosols are presented in Tables 1–3. The spectral aerosol optical depths, single-scattering albedo, real, and imaginary refractive indices exhibit strong seasonal variation and therefore were grouped as follows: (1) the dry season (November–March) and (b) the wet season (July–September). In Table 1 the spectral aerosol optical depths and precipitable water vapor for dry and wet seasons are given and compared with information from other sources. In Table 2 the single-scattering albedo at different wavelengths is illustrated and compared with results from previous studies [*d'Almeida*, 1987; *Carlson and Caverly*, 1977]. In Table 3 the real and imaginary refractive indices are presented for different wavelengths, both for the dry and for the wet seasons. Imaginary refractive indices show high values during the dry season, suggesting an abundance of absorbing aerosols. The present study is based on state of the art observations of accurate Sun and sky measurements, as well as advanced retrieval techniques [*Dubovik and King*, 2000]. It is hoped that the proposed aerosol characteristics will depict more accurately the conditions in this unique region.

4. Summary

Optical characteristics of aerosols observed over Ilorin, Nigeria, are distinctly different during the harmattan, as compared to other seasons. The strong spectral dependence in aerosol optical depths during the dry season indicates an abundance of sub-micron-size particles. During dust storm events, spectral aerosol optical depths were found to have near-neutral extinction, with Angstrom exponents being reduced to 0.3. Precipitable water vapor, which was retrieved using direct Sun measurements at 940 nm [*Bruegge et al.*, 1992], exhibits significant seasonal variation and agrees well with NCEP reanalysis values. Seasonal means of AODs are negatively cor-

related with precipitable water vapor. The proposed size distribution model suggests bimodal/trimodal distribution with a dominant coarse mode. Shift in coarse mode radii and trimodal distribution for higher optical depths (τ_a (670) >1.0) can be noted. The seasonal variation of the single-scattering albedo shows lower values during the dry season, indicating the dominance of aerosols from biomass burning. Despite the lower accuracy in the real and imaginary refractive indices retrieval, the mean values of the spectral real and imaginary refractive indices are close to values reported for silicates and organic species.

References

Adebayo, S. I., Trajectories of advected Saharan dust in Nigeria, *Atmos. Environ.*, *23*, 1581–1589, 1989.

Adedokun, J. A., W. O. Emofurieta, and O. A. Adedeji, Physical, mineralogical and chemical properties of Harmattan dust at Ile-Ife, Nigeria, *Theor. Appl. Climatol.*, *40*, 161–169, 1989.

Adefolalu, D. O., On bioclimatological aspects of Harmattan dust haze in Nigeria, *Arch. Meteorol. Geophys. Bioclimatol. Ser. B*, *33*(4), 387–404, 1984.

Afeti, G. M., and F. J. Resch, Physical characteristics of Saharan dust near the Gulf of Guinea, *Atmos. Environ.*, *34*, 1273–1279, 2000.

Alpert, P., Y. J. Kaufman, Y. Shay-El, D. Tanre, A. da Silva, S. Schubert, and J. H. Joseph, Quantification of dust-forced heating of the lower troposphere, *Nature*, *395*, 367–370, 1998.

American Geophysical Union, The perfect haze: Scientists link 1999 U.S. pollution episode to Midwest aerosol plumes and Kennedy plane crash, *Eos Trans. AGU*, *81*(2), 13–14, 2000.

Bruegge, C. T., J. E. Conel, R. O. Green, J. S. Margolis, R. G. Holm, and G. Toon, Water vapor column abundance retrievals during FIFE, *J. Geophys. Res.*, *97*, 18,759–18,768, 1992.

Carlson, T. N., and R. S. Caverly, Radiative characteristics of Saharan dust at solar wavelengths, *J. Geophys. Res.*, *82*, 3141–3152, 1977.

Carlson, T. N., and J. M. Prospero, The large scale movement of Saharan air outbreaks over the northern equatorial Atlantic, *J. Appl. Meteorol.*, *11*, 283–297, 1972.

Chang, C.-B., Impact of desert environment on the genesis of African wave disturbances, *J. Atmos. Sci.*, *50*, 2137–2145, 1993.

Cox, R. E., M. A. Mazurek, and B. R. T. Simoneit, Lipids in Harmattan aerosols of Nigeria, *Nature*, *296*, 848–849, 1982.

Chowdhary, J., B. Cairns, M. Mishchenko, and L. Travis, Retrieval of aerosol properties over the ocean using multispectral and multiangle photopolarimetric measurements from the Research Scanning Polarimeter, *Geophys. Res. Lett.*, *28*, 243–246, 2001.

d'Almeida, G. A., A model for Saharan dust transport, *J. Clim. Appl. Meteorol.*, *24*, 903–916, 1986.

d'Almeida, G. A., On the variability of desert aerosol radiative characteristics, *J. Geophys. Res.*, *92*, 3017–3026, 1987.

d'Almeida, G. A., P. Koepke, and E. P. Shettle, *Atmospheric Aerosols, Global Climatology and Radiative Characteristics*, 561 pp., A. Deepak, Hampton, Va., 1991.

Dubovik, O., and M. D. King, A flexible inversion algorithm for retrieval of aerosol optical properties from Sun and sky radiance measurements, *J. Geophys. Res.*, *105*, 20,673–20,696, 2000.

Dubovik, O., A. Smirnov, B. N. Holben, M. D. King, Y. J. Kaufman, T. F. Eck, and I. Slutsker, Accuracy assessment of aerosol optical properties retrieval from AERONET Sun and sky radiance measurements, *J. Geophys. Res.*, *105*, 9791–9806, 2000.

Eck, T. F., B. N. Holben, J. S. Reid, O. Dubovik, A. Smirnov, N. T. O'Neill, I. Slutsker, and S. Kinne, Wavelength dependence of the optical depth of biomass burning, urban, and desert dust aerosols, *J. Geophys. Res.*, *104*, 31,333–31,349, 1999.

Faizoun, C. A., A. Podaire, and G. Dedieu, Monitoring of Sahelian aerosol and atmospheric water vapor content characteristics from sun-photometer measurements, *J. Appl. Meteorol.*, *33*, 1291–1304, 1994.

Grams, G. W., I. H. Blifford Jr., D. A. Gillette, and P. B. Russell, Complex index of refraction of airborne soil particles, *J. Appl. Meteorol.*, *13*, 459–471, 1974.

Haywood, J. M., V. Ramaswamy, and B. J. Soden, Tropospheric aerosol climate forcing in clear-sky satellite observations over the oceans, *Science*, *283*, 1299–1303, 1999.

Herman, J. R., and E. Celarier, Earth's surface reflectivity climatology at 340–380 nm from TOMS data, *J. Geophys. Res.*, *102*, 28,003–28,012, 1997.

Holben, B. N., et al., AERONET—A federated instrument network and data archive for aerosol characterization, *Remote Sens. Environ.*, *66*, 1–16, 1998.

Houghton, J. T., L. G. M. Filho, B. A. Callandar, N. Harris, A. Katternberg, and K. Maskell (Eds.), IPCC 95, climate change, in *The Science of Climate Change*, 572 pp., Cambridge Univ. Press, New York, 1996.

Junge, C. E., The size distribution and aging of natural aerosols as determined from electrical and optical data on the atmosphere, *J. Meteorol.*, *12*, 13–25, 1955.

Kalu, A. E., The African dust plume: Its characteristics and propagation across West Africa in winter, in *Saharan Dust*, edited by C. Morales, pp. 95–118, 1979.

Karyampudi, V. M., and T. N. Carlson, Analysis and numerical simulations of the Saharan air layer and its impact on easterly wave disturbances, *J. Atmos. Sci.*, *45*, 3102–3136, 1988.

Karyampudi, V. M., et al., Validation of the Saharan dust plume conceptual model using lidar, Meteosat and ECMWF data, *Bull. Am. Meteorol. Soc.*, *80*, 1045–1075, 1999.

Kaufman, Y. J., Satellite sensing of aerosol absorption, *J. Geophys. Res.*, *92*, 4307–4317, 1987.

Kaufman, Y. J., and R. S. Fraser, The effect of smoke particles on clouds and climate forcing, *Science*, *277*, 1636–1639, 1997.

King, M. D., Y. J. Kaufman, W. P. Menzel, and D. Tanre, Remote Sensing of cloud, aerosol and water vapor properties from the Moderate Resolution Imaging Spectrometer (MODIS), *IEEE Trans. Geosci. Remote Sens.*, *30*, 2–27, 1992.

Koepke, P., M. Hess, I. Schult, and E. P. Shettle, Global Aerosol Data Set (GADS), *MPI Meteorol. Rep. 243*, 44 pp., Max Planck Inst., Hamburg, Germany, 1997.

Krekov, G. M., Models of atmospheric aerosols, in *Aerosol Effects on Climate*, edited by S. G. Jennings, pp. 9–64, 1993.

Lindberg, J. D., and J. B. Gillespie, Relationships between particle size and imaginary refractive index in atmospheric dust, *Appl. Opt.*, *16*, 2628–2630, 1977.

Lindberg, J. D., and L. A. Laude, Measurement of the absorption coefficient of atmospheric dust, *Appl. Opt.*, *13*, 1923–1927, 1974.

McTainsh, G., Harmattan dust deposition in northern Nigeria, *Nature*, *286*, 587–588, 1980.

Mishchenko, M. I., and L. D. Travis, Satellite retrieval of aerosol

properties over the ocean using polarization as well as intensity of reflected sunlight, *J. Geophys. Res.*, *102*, 16,989–17,013, 1997.

Mishchenko, M. I., I. V. Geogdzhayev, B. Cairns, W. B. Rossow, and A. A. Lacis, Aerosol retrievals over the ocean by use of channels 1 and 2 AVHRR data: Sensitivity analysis and preliminary results, *Appl. Opt.*, *38*, 7325–7341, 1999.

Miskolczi, F., T. O. Aro, M. Iziomon, and R. T. Pinker, Surface radiative fluxes in Sub-Sahel Africa, *J. Appl. Meteorol.*, *36*, 521–530, 1997.

Nakajima, T., and A. Higurashi, A use of two-channel radiances for an aerosol characterization from space, *Geophys. Res. Lett.*, *25*, 3815–3818, 1998.

Nicholson, S., Land surface processes and Sahel climate, *Rev. Geophys.*, *38*, 117–139, 2000.

N'Tchayi Mbourou, G. M., J. Bertrand, M. Legrand, and J. Baudet, Temporal and spatial variations of the atmospheric dust loading throughout West Africa over the last thirty years, *Ann. Geophys.*, *12*, 265–273, 1994.

N'Tchayi Mbourou, G. M., J. Bertrand, and S. E. Nicholson, The diurnal and seasonal cycles of wind-borne dust over Africa north of the equator, *J. Appl. Meteorol.*, *36*, 868–882, 1997.

Ohmura, A., et al., *Bull. Am. Meteorol. Soc.*, *79*, 2115–2136, 1998.

Pandithurai, G., P. C. S. Devara, P. E. Raj, and S. Sharma, Retrieval of aerosol size index from high-resolution spectroradiometer observations, *Aerosol Sci. Technol.*, *26*, 154–162, 1997.

Patterson, E. M., D. A. Gillette, and B. H. Stockton, Complex index of refraction between 300 and 700 nm for Saharan aerosols, *J. Geophys. Res.*, *82*, 3153–3160, 1977.

Pinker, R. T., G. Idemudia, and T. O. Aro, Characteristic aerosol optical depths during the Harmattan season in sub-Sahara Africa, *Geophys. Res. Lett.*, *21*, 1099–1103, 1994.

Pinker, R. T., G. Pandithurai, B. N. Holben, O. Dubovik, and T. O. Aro, A dust outbreak episode in sub-Sahel West Africa, *J. Geophys. Res.*, in press, 2001.

Prospero, J. M., Long-term measurements of the transport of African mineral dust to the southeastern United States: Implications for regional air quality, *J. Geophys. Res.*, *104*, 15,917–15,927, 1999.

Rangarajan, S., Wavelength exponent for haze scattering in the tropics as determined by photoelectric photometers, *Tellus*, *24*, 51–59, 1972.

Reid, J. S., T. F. Eck, S. A. Christopher, P. V. Hobbs, and B. N. Holben, Use of the Angstrom exponent to estimate the variability of optical and physical properties of aging smoke particles in Brazil, *J. Geophys. Res.*, *104*, 27,473–27,489, 1999.

Remer, L. A., Y. J. Kaufman, and B. N. Holben, Interannual variation of ambient aerosol characteristics on the east coast of the United States, *J. Geophys. Res.*, *104*, 2223–2231, 1999.

Shettle, E. P., Optical and radiative properties of a desert aerosol model, in *Proceedings of the Symposium on Radiation in the Atmosphere*, edited by G. Fiocco, pp. 74–77, A. Deepak, Hampton, Va., 1984.

Sokolik, I. N., and O. B. Toon, Incorporation of mineralogical composition into models of the radiative properties of mineral aerosol from UV to IR wavelengths, *J. Geophys. Res.*, *104*, 9423–9444, 1999.

Stowe, L. L., A. M. Ignatov, and R. R. Singh, Development, validation, and potential enhancements to the second-generation operational aerosol product at the National Environmental Satellite, Data, and Information Service of the National Oceanic and Atmospheric Administration, *J. Geophys. Res.*, *102*, 16,923–16,934, 1997.

Tegen, I., and I. Fung, Modeling of mineral dust in the atmosphere: Sources, transport, and optical thickness, *J. Geophys. Res.*, *99*, 22,897–22,914, 1994.

Tegen, I., and I. Fung, Contribution to the atmospheric mineral aerosol load from land surface modification, *J. Geophys. Res.*, *100*, 18,707–18,726, 1995.

Tegen, I., and R. Miller, A general circulation model study on the interannual variability of soil dust aerosol, *J. Geophys. Res.*, *103*, 25,975–25,995, 1998.

Tegen, I., P. Hollrig, M. Chin, I. Fung, D. Jacob, and J. Penner, Contribution of different aerosol species to the global aerosol extinction optical thickness: Estimates from model results, *J. Geophys. Res.*, *102*, 23,895–23,915, 1997.

Torres, O., P. K. Bhartia, J. R. Herman, Z. Ahmad, and J. Gleason, Derivation of aerosol properties from satellite measurements of backscattered ultraviolet radiation: Theoretical basis, *J. Geophys. Res.*, *103*, 17,099–17,110, 1998.

Tuller, S. E., World distribution of mean monthly and annual precipitable water, *Mon. Weather Rev.*, *96*, 785–797, 1968.

Wendish, M., and W. von Hoyningen-Huene, Possibility of refractive index determination of atmospheric aerosol particles by ground-based solar extinction and scattering measurements, *Atmos. Environ.*, *28*, 785–792, 1994.

Westphal, D. L., O. B. Toon, and T. N. Carlson, A case study of mobilization and transport of Saharan dust, *J. Atmos. Sci.*, *45*, 2145–2175, 1988.

Wilson, I. G., Desert sand flow basins and a model for the development of ERGS, *Geograph. J.*, *137*, 180–199, 1971.

Wilson, R., and J. Spengler (Eds.), *Particles in Our Air: Concentrations and Health Effects*, 254 pp., Harvard Univ. Press, Cambridge, Mass., 1996.

Yamasoe, M. A., Y. J. Kaufman, O. Dubovik, L. A. Remer, B. N. Holben, and P. Artaxo, Retrieval of the real part of the refractive index of smoke particles from Sun/sky measurements during SCAR-B, *J. Geophys. Res.*, *103*, 31,893–31,902, 1998.

———————————

T. O. Aro, University of Ilorin, Ilorin, Nigeria.

O. Dubovik and B. N. Holben, Laboratory for Terrestrial Physics, NASA Goddard Space Flight Center, Code 923, Greenbelt, MD 20771.

G. Pandithurai and R. T. Pinker, Department of Meteorology, University of Maryland, College Park, MD 20742, USA. (pinker@atmos.umd.edu)